Multiphysics Modeling of Composite Beams under Large Temperature Changes

Qi Wang*
and
Wenbin Yu†
Utah State University, Logan, Utah 84322-4130

Previously developed VABS multiphysics beam model as presented on last SDM is extended to incorporate temperature-dependent materials experiencing large temperature changes. In this study, a new thermomechanical model has been developed for heterogeneous composite materials which removed the restriction on temperature variations and added the dependence of material properties with respect to temperature based on the Kovalenoko's small-strain thermoelasticity theory. In order to avoid ill-conditioned matrix in multiphysics modeling, a scaling method is presented. Numerical example is provided to show the effect of material temperature-dependency. The pyroelectric and pyromagnetic effects are also discussed.

Introduction

Multiphysics modeling mainly deals with the behavior of engineering structures composed of smart materials working under multiple physical fields: mechanical, thermal, electric and magnetic. Smart materials are defined as those that exhibit coupling between multiple physical domains.[1–5] A well-known smart material is piezoelectric, which creates conversion interface between electrical energy and mechanical energy. As an analogy with the exhibition of electromechanical coupling of piezoelectric materials, magnetic materials respond to an externally applied magnetic field by exhibiting a shape change which is known as magnetostriction, demonstrating the Joule effect. On the other hand, these magnetic materials also demonstrate the Villari effect indicated by changing their magnetization and consequently the magnetic induction in response to the applied stress.[6–10] Recently, the newly developed composites contain both piezoelectric phase and piezomagnetic phase exhibit a magnetoelectric coupling effect which does not exist in either of the two constitutive phases. Structures composed of these smart materials, often function as actuators and sensors, are usually called "smart structures". Applications of the smart structure include vibration suppression,[11] shape control[12] and aeroelastic stability augmentation.[13]

Due to their special characteristics like high-strength, light-weighted, and self-controlling, the composite beam structure often works under extreme conditions in aerospace systems. For example, the thermal protection system of space vehicles has to withstand temperatures ranging from 300°C to 1500°C during ascent and reentry, while in the outer space, the vehicle surface may be subjected to temperatures up to −150°C.[14] Moreover, composite materials are more sensitive and vulnerable to temperature change than their isotropic counterparts. For composites, the thermal expansion coefficients of different constituents of the material are usually dramatically different from each other resulting in high stresses due to temperature changes from stress free environment. The difficulty of thermal analysis of smart structure is compounded by other two factors. For one thing, the mechanical response of smart structure is coupled with the non-mechanical effects. For example, the structure containing piezoelectric materials can exhibit mechanical-electric coupling

*Graduate Research Assistant, Department of Mechanical and Aerospace Engineering. Student Member, AIAA
†Associate Professor, Department of Mechanical and Aerospace Engineering. Senior Lifetime Member, AIAA; Member, ASME and AHS.

and pyroelectric effect, and as an analogy, piezomagnetic material can exhibit mechanical-magnetic coupling and pyromagnetic effect. For another, the traditional constitutive framework of thermoelasticity which is based on temperature-independent condition, small temperature assumption, and small strain assumption may not work for structures experiencing large temperature changes. For most cases, it is still reasonable to assume the strains are small. However, The temperature change cannot be considered as "small". And also, if the temperature changes are large enough, the material properties including elastic constants, coefficients of thermal expansion become temperature dependent.[15,16]

Various forms of constitutive equations and variational principles for magneto-electro-elastic solids were derived in Refs. [17–21]. The open literature relevant to the analysis of electromagnetoelastic beam structure is rather scanty. Jiang and Ding[22] presented an analytical solution to magneto-electro-elastic beams with different boundary conditions. Kumaravel *et al.*[23] investigated a three-layered electro-magneto-elastic strip under a plane stress condition. The thermal loading conditions, including uniform temperature rise and non-uniform temperature distribution, were considered. Two types of stacking sequence of the laminate beam under different boundary conditions were studied. Davì *et al.*[10] analyzed magneto-electro-elastic bimorph beams using a boundary element approach.

Recently, the variational asymptotic method (VAM) proposed by Berdichevsky[24] is introduced as a viable alternative approach to model smart composite beams without invoking apriori assumptions.[25–31] Taking advantage of the smallness of aspect ratio of beams, we can use VAM to decouple the original 3D nonlinear problem into two sets of analyses: two-dimensional (2D), linear, cross-sectional analysis and one-dimensional (1D), nonlinear global beam analysis. This allows the global beam analysis to be formulated exactly and intrinsically as a general 1D continuum over the reference line and confines all approximations to the cross-sectional analysis, the accuracy of which is guaranteed to be the best by VAM. In the present research, we will apply VAM to construct a geometrically nonlinear beam model for multiphysics analysis considering temperature-dependent material properties and finite temperature changes. The pyroelectric and pyromagnetic effects will be studied in the numerical examples.

Finite Temperature Change Small Strain Thermoelasticity

To relax the assumption of small temperature changes, we need to derive a Helmholtz free energy suitable for materials with temperature dependent properties and experiencing finite temperature changes. This implies that we need first to define the material properties of interest as temperature dependent, such as the coefficient of thermal expansion $\alpha(\sigma_{ij}, T)$, the elastic constants $C_{ijkl}(T)$, the thermal strain tensor $m(T)$, and the thermal stress tensor $l(T)$ and etc. The symbol outside the parenthesis denotes the physical quantity while the symbols inside parenthesis are regarded as the independent variables used to describe the state of function. Note that for a defined function $F(\sigma_{ij}, T)$ or $F(\epsilon_{ij}, T)$, the quantity $F(0, T)$ means $F(\sigma_{ij} = 0, T)$(constant stress state) or $F(\epsilon_{ij} = 0, T)$(constant strain state) depending on how the function is defined.

The Helmholtz free energy density $f(\epsilon_{ij}, T)$ is a function of strain field ϵ_{ij} and the absolute temperature T. Let us not put any restriction on T but assuming ϵ_{ij} to be small, then we can carry out a Taylor expansion of $f(\epsilon_{ij}, T)$ in terms of the small strain field, ϵ_{ij}, as

$$f(\epsilon_{ij}, T) = f(0, T) + \epsilon_{ij}\frac{\partial f(\epsilon_{ij}, T)}{\partial \epsilon_{ij}}|_{\epsilon_{ij}=0} + \frac{1}{2}\epsilon_{ij}\epsilon_{kl}\frac{\partial^2 f(\epsilon_{ij}, T)}{\partial \epsilon_{ij}\partial \epsilon_{kl}}|_{\epsilon_{ij}=0} \tag{1}$$

Here only up to the quadratic terms of the strain field are kept due the assumption of small strains. As the constant term $f(0, T)$ will not affect our thermoelastic analysis,[32] the constant term $f(0, T)$ is dropped. We know $\sigma_{ij} = \frac{\partial f}{\partial \epsilon_{ij}}$, that is

$$\sigma_{ij} = C_{ijkl}(T)\epsilon_{kl} + l_{ij}(T) \tag{2}$$

with $C_{ijkl}(T) = \frac{\partial^2 f(\epsilon_{ij}, T)}{\partial \epsilon_{ij}\partial \epsilon_{kl}}|_{\epsilon_{ij}=0}$ as the fourth-order elasticity tensor and $l_{ij}(T) = \frac{\partial f(\epsilon_{ij}, T)}{\partial \epsilon_{ij}}|_{\epsilon_{ij}=0}$ as the second-order thermal stress tensor. We can also rewrite the stress-strain relations as

$$\epsilon_{ij} = S_{ijkl}(T)\sigma_{kl} + m_{ij}(T) \tag{3}$$

with S_{ijkl} as the fourth-order compliance tensor and m_{ij} as the second-order thermal strain tensor and we have $m_{ij} = -S_{ijkl}l_{kl}$. The coefficients of thermal expansion, α_{ij}, as a function of stress field and temperature,

is defined as

$$\alpha_{ij} = \frac{\partial \epsilon_{ij}}{\partial T}|_{\sigma_{ij}=\text{constant}} \tag{4}$$

Then from Eq. (3) and (4), we have

$$\alpha_{ij} = S'_{ijkl}\sigma_{kl} + m'_{ij} \tag{5}$$

where prime is used to denote derivative with respect to T, *i.e.*, $m'_{ij} = \frac{dm_{ij}}{dT}$. From Eq. (5), we have

$$\alpha_{ij}(0,T) = m'_{ij} \tag{6}$$

where we can obtain

$$m_{ij} = \int_{T_0}^{T} \alpha_{ij}(0,\zeta)d\zeta + m_{ij}(T_0) \tag{7}$$

Note here $\alpha_{kl}(0,T)$ are the stress-free coefficients of thermal expansion which can be easily measured at a specific temperature T. We normally choose our reference state to be at $T = T_0$ with stress and strain free, which implies $m_{ij}(T_0) = 0$ in view of Eq. (3). Then we can express our thermal strain tensor in a form similar as that we used for small temperature variations

$$m_{ij} = \check{\alpha}_{ij}(T)\theta \quad \text{with} \quad \check{\alpha}_{ij}(T) = \frac{1}{\theta}\int_{T_0}^{T_0+\theta} \alpha_{ij}(0,\zeta)d\zeta \tag{8}$$

Here $\theta = T - T_0$ denotes the temperature change from the reference temperature. Normally, $\check{\alpha}_{ij}(T)$ is termed as the secant free thermal expansion coefficients. We can also express the thermal stress tensor as

$$l_{ij}(T) = -C_{ijkl}(T)m_{kl}(T) = -C_{ijkl}(T)\check{\alpha}_{ij}(T)\theta \equiv \check{\beta}_{ij}(T)\theta \tag{9}$$

Here, $\check{\beta}_{ij}(T)$ can be similarly called secant free thermal stress coefficients.

Substituting Eq. (9) into Eq. (1), we have the Helmholtz energy for thermoelastic analysis considering the temperature-dependent material properties without assuming small temperature changes as

$$f(\epsilon_{ij},T) = \frac{1}{2}C_{ijkl}\epsilon_{ij}\epsilon_{kl} + \check{\beta}_{ij}(T)\epsilon_{ij}\theta \tag{10}$$

Variational Asymptotic Multiphysics Modeling of Composite Beams

For structures active to electromagnetic fields, the internal energy is the extended Helmholtz free energy containing contributions from mechanical, electric, magnetic and thermal fields and the coupling effects among them

$$\begin{aligned}\mathcal{U}_A =& \frac{1}{2}\int_{\mathcal{V}} [\,\boldsymbol{\Gamma} : \boldsymbol{C}^{\boldsymbol{E},\boldsymbol{H}} : \boldsymbol{\Gamma} - \boldsymbol{E}\cdot\boldsymbol{k}^{\boldsymbol{\Gamma},\boldsymbol{H}}\cdot\boldsymbol{E} - \boldsymbol{H}\cdot\boldsymbol{\mu}^{\boldsymbol{\Gamma},\boldsymbol{E}}\cdot\boldsymbol{H} \\ & - 2\boldsymbol{E}\cdot\boldsymbol{e}^{H} : \boldsymbol{\Gamma} - 2\boldsymbol{H}\cdot\boldsymbol{q}^{E} : \boldsymbol{\Gamma} - 2\boldsymbol{E}\cdot\boldsymbol{a}^{\Gamma}\cdot\boldsymbol{H} - 2(\boldsymbol{\Gamma} : \boldsymbol{\Lambda} + \boldsymbol{E}\cdot\boldsymbol{p} + \boldsymbol{H}\cdot\boldsymbol{m})\cdot\theta\,]\,\mathrm{d}\mathcal{V}\end{aligned} \tag{11}$$

where $\boldsymbol{\Gamma}$, $\boldsymbol{E}$ and $\boldsymbol{H}$ are the strain, electric field and magnetic field tensors, respectively; $\boldsymbol{e}^H$, $\boldsymbol{q}^E$ and $\boldsymbol{a}^\Gamma$ are piezoelectric tensor (measured at constant magnetic field), piezomagnetic tensor (measured at constant electric field) and magnetoelectric tensor (measured at constant strain), respectively; $\boldsymbol{C}^{E,H}$, $\boldsymbol{k}^{\boldsymbol{\Gamma},\boldsymbol{H}}$ and $\boldsymbol{\mu}^{\boldsymbol{\Gamma},\boldsymbol{E}}$ are elastic tensor (measured at constant electric and magnetic field), dielectric tensor (measured at constant strain and magnetic field) and magnetic permeability tensor (measured at constant strain and electric field), respectively; $\boldsymbol{\Lambda}$, $\boldsymbol{p}$ and $\boldsymbol{m}$ are thermal stress tensor (which is defined as $\boldsymbol{\Lambda} = \boldsymbol{C}^{E,H} : \boldsymbol{\alpha}$ with $\boldsymbol{\alpha}$ the coefficients of thermal expansion), pyroelectric vector and pyromagnetic vector, respectively; θ denotes the difference between the actual temperature and the reference temperature; $\mathcal{V}$ is the space occupied by the structure.

The differential form of the constitutive equations can be expressed as

$$\begin{aligned}\sigma_{ij} &= C_{ijkl}\Gamma_{kl} - e_{kij}E_k - q_{kij}H_k - \Lambda_{ij}\theta \\ D_i &= e_{ikl}\Gamma_{kl} + k_{ik}E_k + a_{ik}H_k + p_i\theta \\ B_i &= q_{ikl}\Gamma_{kl} + a_{ik}E_k + \mu_{ik}H_k + m_i\theta\end{aligned} \tag{12}$$

where σ_{ij}, Γ_{ij}, D_i, and B_i are the stress tensor, strain tensor, electric displacement, and magnetic induction, respectively. In the present study, we does not restrict θ to be small as we have discussed in the previous section. If θ is not small, Λ_{ij}, p_i, m_i are not the tangent or instantaneous properties, but the secant properties which are defined as average over a change of temperature. For example, let $\alpha_t(T)$ denote the tangent or instantaneous coefficient of thermal expansion (CTE), the secant CTE is defined as

$$\alpha(T_i) = \frac{1}{T_i - T_1} \int_{T_1}^{T_i} \alpha_t(\zeta) d\zeta \tag{13}$$

with T_1 as the reference temperature and $\alpha(T_1) = \alpha_t(T_1)$.

As shown in Ref. [31], the extended Helmholtz free energy can be expressed as

$$\begin{aligned} \mathcal{U}_A &= \frac{1}{2} \int_0^L \left\langle \left\langle \hat{\Gamma}^T \bar{D} \hat{\Gamma} - 2\hat{\Gamma}^T \beta\theta \right\rangle \right\rangle dx_1 \\ &\equiv \frac{1}{2} \int_0^L U_A dx_1 \end{aligned} \tag{14}$$

where L denotes the length of the beam, $\hat{\Gamma}$ is the extended Jaumann-Biot-Cauchy strains defined as

$$\hat{\Gamma} = \lfloor \Gamma_{11} \;\; 2\Gamma_{12} \;\; 2\Gamma_{13} \;\; \Gamma_{22} \;\; 2\Gamma_{23} \;\; \Gamma_{33} \;\; E_1 \;\; E_2 \;\; E_3 \;\; H_1 \;\; H_2 \;\; H_3 \rfloor^T \tag{15}$$

The notation $\langle\langle \bullet \rangle\rangle = \int_s \bullet \sqrt{g}\, \mathrm{d}x_2\, \mathrm{d}x_3$. $\bar{D}$ is a 12×12 multiphysics matrix, which we term it as the generalized stiffness matrix, containing all the necessary material constants for characterizing fully coupled thermoelectromagnetoelastic materials such that

$$\bar{D} = \begin{bmatrix} C & -e & -q \\ -e^T & -k & -a \\ -q^T & -a^T & -\mu \end{bmatrix} \tag{16}$$

where C is a 6×6 submatrix for elastic constants, e is a 6×3 submatrix for piezoelectric coefficients, q is a 6×3 submatrix for piezomagnetic coefficients, k is a 3×3 submatrix for dielectric coefficients, a is a 3×3 submatrix for electromagnetic coefficients, and μ is a 3×3 submatrix for magnetic permeability. To avoid confusion, we provide the explicit form of the 12×12 matrix as follows

$$\begin{bmatrix} c_{11} & c_{12} & c_{13} & c_{14} & c_{15} & c_{16} & -e_{11} & -e_{21} & -e_{31} & -q_{11} & -q_{21} & -q_{31} \\ c_{12} & c_{22} & c_{23} & c_{24} & c_{25} & c_{26} & -e_{12} & -e_{22} & -e_{32} & -q_{12} & -q_{22} & -q_{32} \\ c_{13} & c_{23} & c_{33} & c_{34} & c_{35} & c_{36} & -e_{13} & -e_{23} & -e_{33} & -q_{13} & -q_{23} & -q_{33} \\ c_{14} & c_{24} & c_{34} & c_{44} & c_{45} & c_{46} & -e_{14} & -e_{24} & -e_{34} & -q_{14} & -q_{24} & -q_{34} \\ c_{15} & c_{25} & c_{35} & c_{45} & c_{55} & c_{56} & -e_{15} & -e_{25} & -e_{35} & -q_{15} & -q_{25} & -q_{35} \\ c_{16} & c_{26} & c_{36} & c_{46} & c_{56} & c_{66} & -e_{16} & -e_{26} & -e_{36} & -q_{16} & -q_{26} & -q_{36} \\ -e_{11} & -e_{12} & -e_{13} & -e_{14} & -e_{15} & -e_{16} & -k_{11} & -k_{12} & -k_{13} & -a_{11} & -a_{12} & -a_{13} \\ -e_{21} & -e_{22} & -e_{23} & -e_{24} & -e_{25} & -e_{26} & -k_{12} & -k_{22} & -k_{23} & -a_{21} & -a_{22} & -a_{23} \\ -e_{31} & -e_{32} & -e_{33} & -e_{34} & -e_{35} & -e_{36} & -k_{13} & -k_{23} & -k_{33} & -a_{31} & -a_{32} & -a_{33} \\ -q_{11} & -q_{12} & -q_{13} & -q_{14} & -q_{15} & -q_{16} & -a_{11} & -a_{21} & -a_{31} & -\mu_{11} & -\mu_{12} & -\mu_{13} \\ -q_{21} & -q_{22} & -q_{23} & -q_{24} & -q_{25} & -q_{26} & -a_{12} & -a_{22} & -a_{32} & -\mu_{12} & -\mu_{22} & -\mu_{23} \\ -q_{31} & -q_{32} & -q_{33} & -q_{34} & -q_{35} & -q_{36} & -a_{13} & -a_{23} & -a_{33} & -\mu_{13} & -\mu_{23} & -\mu_{33} \end{bmatrix} \tag{17}$$

Other terms in Eq. (14) include β, which is a 12×1 matrix containing the second-order thermal stress tensor Λ_{ij}, the vector of pyroelectric p_i, and the vector of pyromagnetic m_i expressed as

$$\beta = \lfloor \Lambda_{11} \;\; \Lambda_{12} \;\; \Lambda_{22} \;\; \Lambda_{13} \;\; \Lambda_{23} \;\; \Lambda_{33} \;\; -p_1 \;\; -p_2 \;\; -p_3 \;\; -m_1 \;\; -m_2 \;\; -m_3 \rfloor^T$$

As it is a constant confusion regarding the units used in the multiphysics modeling, we will provide a detailed description of those units. According to the International Standard unit system, we use **Pa** (*i.e.*, $\mathbf{N/m^2}$) for the elastic constants C_{ijkl} and the stress field σ_{ij} (note the strain field Γ_{ij} is unitless), $\mathbf{C/m^2}$

for piezoelectric constants e_{ijk} and electric displacement D_i, $\mathbf{N/(A{\cdot}m)}$ for piezomagnetic constants q_{ijk} and magnetic induction B_i, $\mathbf{C/(V{\cdot}m)}$ for dielectric constants k_{ij}, $\mathbf{N/A^2}$ (or $\mathbf{N{\cdot}s^2/C^2}$) for magnetic permeability μ_{ij}, $\mathbf{C/(A{\cdot}m)}$ for electromagnetic coefficients a_{ij}, $\mathbf{V/m}$ for electric field E_i, $\mathbf{A/m}$ for magnetic field H_i, $\mathbf{K}$ for the temperature field θ (note $^\circ\mathbf{C}$ has the same unit dimension as $\mathbf{K}$), $\mathbf{1/K}$ for thermal expansion coefficients α_{ij} (correspondingly $\mathbf{Pa/K}$ for thermal stress coefficients Λ_{ij}), $\mathbf{C/m^2{\cdot}K}$ for pyroelectric constants p_i, and $\mathbf{N/(A{\cdot}m{\cdot}K)}$ for pyromagnetic m_i. With all these units, the energy density U will be in the unit of $\mathbf{N/m^2}$, which is the same as $\mathbf{J/m^3}$.

Although the units aforementioned are consistent with each other, direct use of these units will introduce an extremely ill-conditioned generalized stiffness matrix $\bar{D}$ as for regular materials, we will have C_{ijkl} in the order of 10^{11}, while k_{ij} in the order of 10^{-9}. Proper scaling is needed even if double precision is used in computing. To this end, we define $E_i^* = 10^{-9}E_i, H_i^* = 10^{-9}H_i$, then the energy density U_A in Eq. (14) can be rewritten as

$$\frac{U_A}{10^9} = \frac{1}{2}\begin{Bmatrix}\Gamma\\E^*\\H^*\end{Bmatrix}^T\begin{bmatrix}C^* & -e & -q\\-e^T & -k^* & -a^*\\-q^T & -a^{*T} & -\mu^*\end{bmatrix}\begin{Bmatrix}\Gamma\\E^*\\H^*\end{Bmatrix} + \begin{Bmatrix}\Gamma\\E^*\\H^*\end{Bmatrix}^T\begin{Bmatrix}-C^*\alpha\\-p\\-m\end{Bmatrix}\theta \tag{18}$$

with

$$C^* = \frac{C}{10^9} \qquad a^* = a\times 10^9 \qquad k^* = k\times 10^9 \qquad \mu^* = \mu\times 10^9 \tag{19}$$

The generalized Hooke's law given in Eq. (12) can be rewritten in the following matrix form

$$\begin{aligned}\sigma^* &= C^*\Gamma - eE^* - qH^* - \Lambda^*\theta\\ D &= e^T\Gamma + k^*E^* + a^*H^* + p_i\theta\\ B &= q^T\Gamma + a^{*T}E^* + \mu^*H^* + m_i\theta\end{aligned} \tag{20}$$

with $\sigma^* = \frac{\sigma}{10^9}$. For VABS multiphysics constitutive modeling, we input $C^*, e, q, k^*, a^*, \mu^*, \alpha, p, m$ as material properties, and for the recovery, we input Γ, E^*, H^* as the field vectors. In other words, the quantities are given in IS units, we need to divide C, E, H by 10^9, and multiply k, a, μ by 10^9, and all the other quantities remain the same. The output effective properties are also scaled the same way as the input material properties. As far as the recovered field concerned, the displacements, electromagnetic potentials, strains, electric displacements, and magnetic induction are the same as SI units, one needs to multiply the stresses, electric and magnetic fields with 10^9 to convert these quantities in SI units. It is pointed out that it is just one suggestion to scale the inputs to avoid numerical difficulties. This scaling is done externally by the end user. One can certainly devise a different scaling following the same philosophy.

There are two types of load types for the applied electric or magnetic field.

- Case 1: Electric or magnetic field is not prescribed at any point over the cross-section, for example, if only the end surfaces at $x_1 = 0$ and $x_1 = L$ have prescribed potential (see Figure 1).

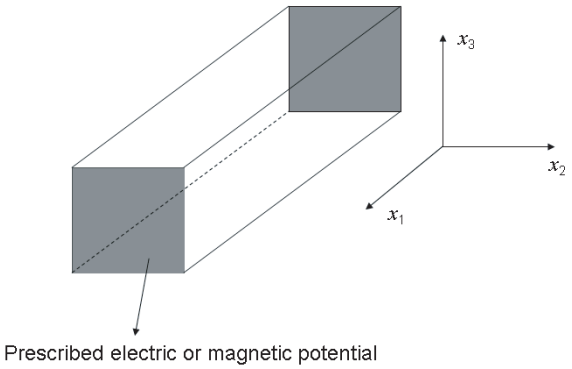

Figure 1: Case 1: electric or magnetic potential prescribed at the end surfaces of the beam.

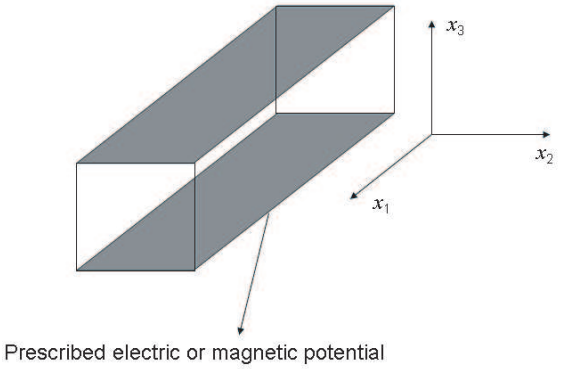

Figure 2: Case 2: electric or magnetic potential prescribed at some points over the cross-section.

- Case 2: Electric or magnetic field is prescribed at some points over the cross-section (see Figure 2).

Two 1D beam models have been constructed in Ref. [31] for these load types. For simplicity, we will only provide these two models but abridge the derivation here with the understanding that the calculation of free thermal stress coefficients is different for temperature-dependent materials. The 1D constitutive relations for a generalized Timoshenko model can be written as

$$\begin{bmatrix} F_1 \\ F_2 \\ F_3 \\ M_1 \\ M_2 \\ M_3 \\ \bar{F}_E \\ \bar{F}_H \end{bmatrix} = \begin{bmatrix} s_{11} & s_{12} & s_{13} & s_{14} & s_{15} & s_{16} & \bar{e}_{11} & \bar{q}_{11} \\ s_{12} & s_{22} & s_{23} & s_{24} & s_{25} & s_{26} & \bar{e}_{12} & \bar{q}_{12} \\ s_{13} & s_{23} & s_{33} & s_{34} & s_{35} & s_{36} & \bar{e}_{13} & \bar{q}_{13} \\ s_{14} & s_{24} & s_{34} & s_{44} & s_{45} & s_{46} & \bar{e}_{14} & \bar{q}_{14} \\ s_{15} & s_{25} & s_{35} & s_{45} & s_{55} & s_{56} & \bar{e}_{15} & \bar{q}_{15} \\ s_{16} & s_{26} & s_{36} & s_{46} & s_{56} & s_{66} & \bar{e}_{16} & \bar{q}_{16} \\ \bar{e}_{11} & \bar{e}_{12} & \bar{e}_{13} & \bar{e}_{14} & \bar{e}_{15} & \bar{e}_{16} & \bar{k}_{77} & \bar{a} \\ \bar{q}_{11} & \bar{q}_{12} & \bar{q}_{13} & \bar{q}_{14} & \bar{q}_{15} & \bar{q}_{16} & \bar{a} & \bar{\mu}_{88} \end{bmatrix} \begin{bmatrix} \gamma_{11} \\ \gamma_{12} \\ \gamma_{13} \\ \kappa_1 \\ \kappa_2 \\ \kappa_3 \\ E_{1D} \\ H_{1D} \end{bmatrix} - \begin{bmatrix} f_1^a \\ f_2^a \\ f_3^a \\ m_1^a \\ m_2^a \\ m_3^a \\ f_E^a \\ f_H^a \end{bmatrix} \tag{21}$$

and

$$\begin{bmatrix} F_1 \\ F_2 \\ F_3 \\ M_1 \\ M_2 \\ M_3 \end{bmatrix} = \begin{bmatrix} s_{11} & s_{12} & s_{13} & s_{14} & s_{15} & s_{16} \\ s_{12} & s_{22} & s_{23} & s_{24} & s_{25} & s_{26} \\ s_{13} & s_{23} & s_{33} & s_{34} & s_{35} & s_{36} \\ s_{14} & s_{24} & s_{34} & s_{44} & s_{45} & s_{46} \\ s_{15} & s_{25} & s_{35} & s_{45} & s_{55} & s_{56} \\ s_{16} & s_{26} & s_{36} & s_{46} & s_{56} & s_{66} \end{bmatrix} \begin{bmatrix} \gamma_{11} \\ \gamma_{12} \\ \gamma_{13} \\ \kappa_1 \\ \kappa_2 \\ \kappa_3 \end{bmatrix} - \begin{bmatrix} f_1^a \\ f_2^a \\ f_3^a \\ m_1^a \\ m_2^a \\ m_3^a \end{bmatrix} \tag{22}$$

for Case 1 and Case 2, respectively.

Numerical Examples

Example 1: Thermoelastic Analysis of a Composite Beam Under Finite Temperature Change

In this section, a cantilever two-layer composite beam is used to examine the temperature-dependent properties and the framework of thermoelasticity based on finite temperature change. Two load cases are studied here, one is the beam under small temperature change and the other is the beam experiencing finite temperature change. The geometry is given by Fig. 3 with the dimensions $L = 1$ m, $b = 0.1$ m, and $t = 0.05$ m. The material properties are listed in Table 1. Firstly, the beam is experiencing a small temperature change, from 480°C to 500°C. The stress distributions of mid-span along thickness are plotted in Fig. 4. The curves and data points labeled "Inst" are calculated based on the traditional framework of thermoelasticity where instantaneous CTEs are used. The curves and data points labeled "Sect" are from the current framework of thermoelasticity where secant CTEs are used in the analysis. Excellent agreement exists between predictions

from VABS and ANSYS 3D analysis. Moreover, due to the load chosen, the newly developed framework of finite temperature change thermoelasticity does not have a huge impact on the results. In other words, the predictions from traditional constitutive framework of thermoelasticity may be adequate for this case.

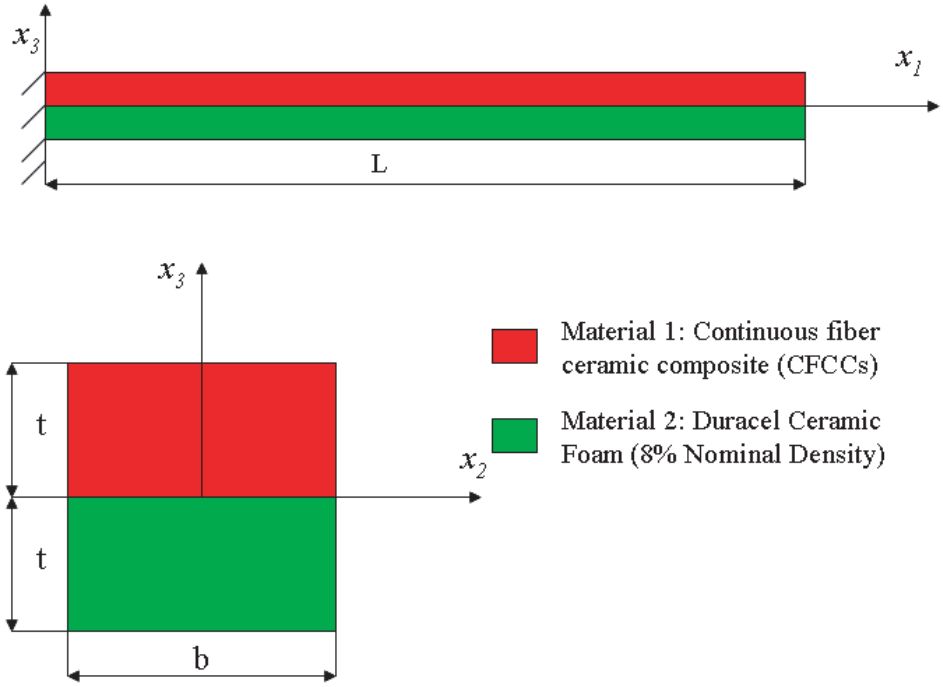

Figure 3: Schematic of a two-layer composite beam for finite temperature change analysis.

For the second case, the composite beam is experiencing a large temperature change from 0°C to 500°C. Fig. 5 show the plots of non-zero stress components σ_{11}, σ_{22}, and σ_{33}, respectively. Again, excellent agreements exist between results from 3D analysis and VABS based on different theories. A striking observation from these three figures is that two different frameworks of thermoelasticity result in huge different stress distributions for this case. It demonstrates that the influence of temperature-dependent material properties and framework of thermoelasticity on thermal stresses is quite significant for finite temperature change cases.

Example 2: Thermal Effects in Multiphysics Analysis

This example is to study the effects of thermal load applied to the structure in multiphysics analysis. A cantilevered smart beam of configuration $[0_8/p]$ is presented, see Fig. 6, where p is the piezoelectric layer. The beam is $L = 25.4$ cm long and $b = 2.54$ cm wide, and consists of eight graphite/epoxy layers and a piezoelectric layer where each layer has a thickness of $t = 0.0127$ cm. Representative material properties of a graphite/epoxy composite are used in this case as $E_{11} = 39$GPa, $E_{22} = E_{33} = 8.6$GPa, $G_{12} = G_{13} = 3.8$GPa, $G_{23} = 3.07$GPa, $\nu_{12} = \nu_{13} = 0.28$, $\nu_{23} = 0.4$, $\alpha_{11} = 7.0 \times 10^{-6}/°\text{C}$, $\alpha_{22} = \alpha_{33} = 21.0 \times 10^{-6}/°\text{C}$. The piezoelectric layer is made of PZT-4 material and the properties are listed in Table **??**. The thermal properties for PZT-4 are $\alpha_{11} = \alpha_{22} = 3.8 \times 10^{-6}/°\text{C}$, $\alpha_{33} = 1.2 \times 10^{-6}/°\text{C}$, and $p_1 = p_2 = 0$, $p_3 = -1.7 \times 10^{-4}\text{C/m}^2 \cdot \text{K}$ where p_i are pyroelectric constants. A uniform temperature load of 100°C is applied

Table 1: Material Properties of Two-layer Composite Beam in Fig. 3

	0°C	200°C	500°C
Material 1: CFCCs	$E = 83$GPa, $\nu = 0.27$ $\alpha = 4.28 \times 10^{-6}/°\text{C}$	$E = 82.47$GPa, $\nu = 0.27$ $\alpha = 4.278 \times 10^{-6}/°\text{C}$	$E = 81.67$GPa, $\nu = 0.27$ $\alpha = 4.275 \times 10^{-6}/°\text{C}$
Material 2: DCF	$E = 2.76$GPa, $\nu = 0.22$ $\alpha = 1.22 \times 10^{-6}/°\text{C}$	$E = 2.76$GPa, $\nu = 0.22$ $\alpha = 2.06 \times 10^{-6}/°\text{C}$	$E = 2.76$GPa, $\nu = 0.22$ $\alpha = 2.56 \times 10^{-6}/°\text{C}$

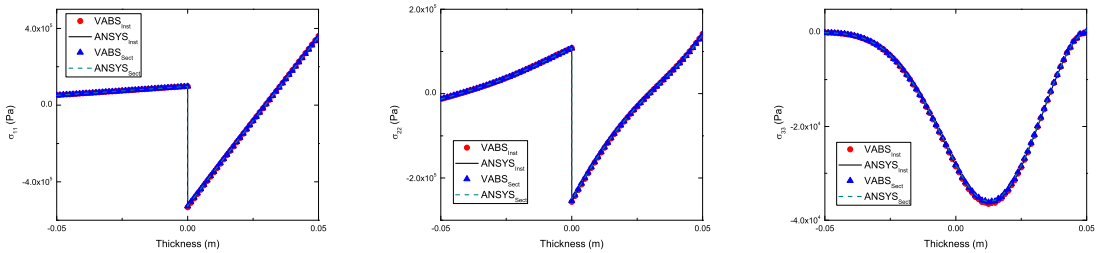

(a) σ_{11} (b) σ_{22} (c) σ_{33}

Figure 4: Distributions of non-zero stress components along the thickness at $x_2 = 0$ for small temperature change.

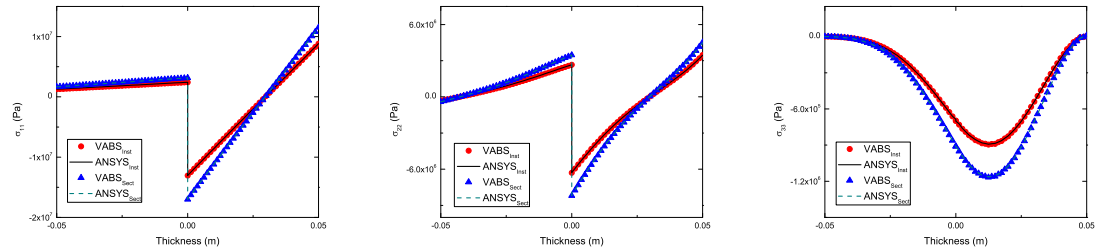

(a) σ_{11} (b) σ_{22} (c) σ_{33}

Figure 5: Distributions of non-zero stress components along the thickness at $x_2 = 0$ for finite temperature change.

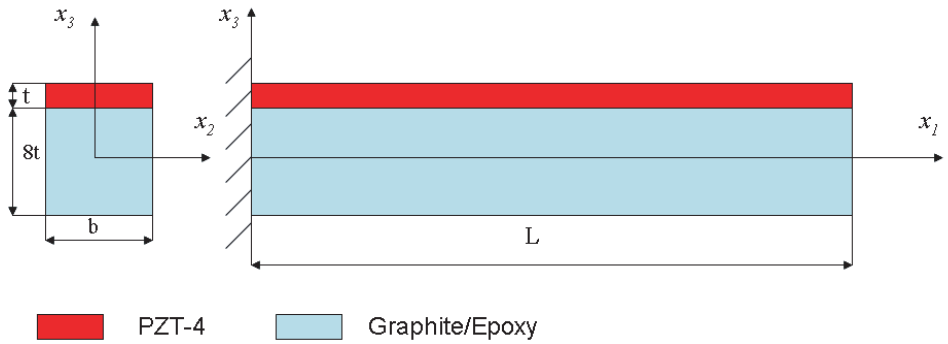

Figure 6: Beam sketch for multiphysics Example 6.

to this beam. The interface between piezoelectric layer and graphite/epoxy layers is grounded and three different electric potentials, 0 V, 100 V, and 300 V, are applied to the top surface of the piezoelectric layer. Fig. 7 shows the transverse displacements caused by thermal and electric loads. These results indicate that the thermally induced deformation can be compensated by piezoelectric actuators when electric loads apply to it. When the piezoelectric layer works in the sensory mode, the deformation of structure can be

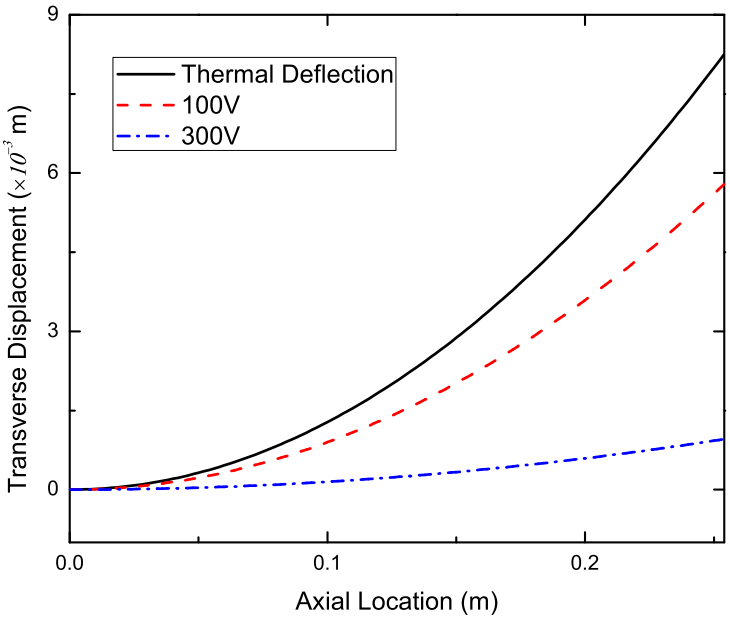

Figure 7: Transverse displacement of a smart beam under thermal-electric loads.

monitored by the electric quantities generated in the layer. Fig. 8 shows the electric displacements detected in the piezoelectric layer under different loads. Firstly, the top surface of the PZT-4 layer is prescribed with a 100 V electric potential and the interface is grounded. The curve and data points labeled "Electric Load" are calculated for this load case from ANSYS 3D coupling analysis and VABS, respectively. Excellent agreement can be observed. Next, a uniform temperature change of 100°C is applied to this beam in addition to the electric load. The curve labeled "Electric-Thermal Load" shows the electric displacement in the PZT-4 layer calculated by VABS. Finally, the electric displacement considering pyroelectric effect under the same electro-thermal load is also plotted in this figure with the label of "Pyroelectric."

Conclusion

In this paper, we proposed a new framework for thermomechanical modeling of compsite beams where the restriction on temperature variations has been removed; and it also takes account for the dependence of material properties with respect to temperature. Starting from a Taylor epansion of Helmholtz free enerengy density, we derived the expression for secant free thermal expansion coefficients only with the small strain assumption. Numerical example shows that the temperature dependency of material properties and thermoelasticity based on the newly developed framework are critical for some case if the structure experiences finite temperature change. We also present a scaling method for multiphysics analysis of composite beams to avoid extremely ill-condidtioned generalized stiffness matrix. The pyroelectric effe ct is demonstrated in a numerical example with studing the distribution of electric displacement inside the multiphysics beam structure.

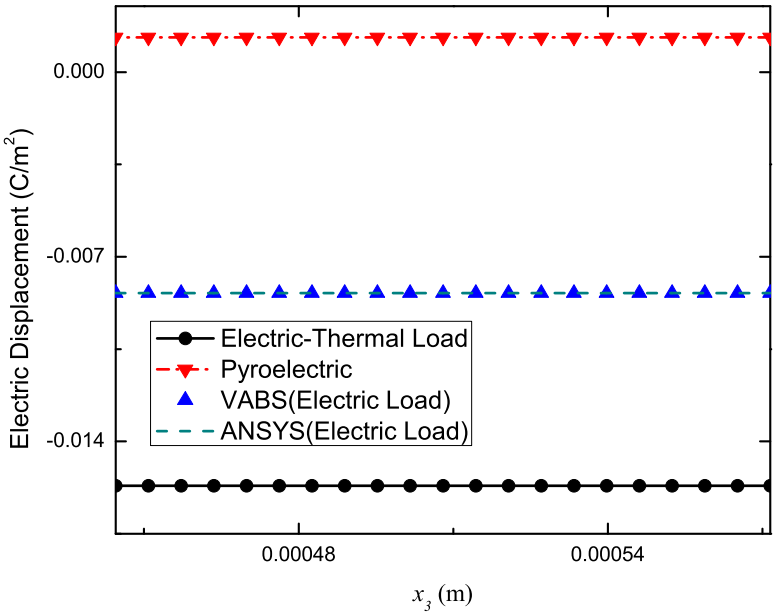

Figure 8: Distribution of electric displacement in the piezoelectric layer for multiphysics Example 2.

Acknowledgment

This research is supported, in part, by the Army Vertical Lift Research Center of Excellence at Georgia Institute of Technology and its affiliate program through subcontract at Utah State University. The technical monitor is Dr. Michael J. Rutkowski.

References

[1]D.A. Berlincourt, D.R. Curran, and H. Jaffe. Piezoelectric and piezomagnetic materials and their function in transducers. *Physical Acoustics*, pages 169–270, 1964.

[2]V.Z. Parton and B.A. Kudryavtsev. *Electromagnetoelasticity, Piezoelectrics and Electrically Conductive Solids.* Gordon & Breach, New York, 1988.

[3]Z.L. Wang and Z.C. Kang. *Functional and Smart Materials.* Plenum Oress, New York, 1998.

[4]G.R. Buchanan. Layered versus multiphase magneto-electro-elastic composites. *Composites Part B: Engineering*, 35:413–420, 2004.

[5]D.J. Leo. *Engineering Analysis of Smart Material Systems.* John Wiley, New York, 2007.

[6]E.T. De Lacheisserie. *Magnetostriction -Theory and Applications of Magnetoelasticity.* CRC Press, Boca Raton, FL, 1993.

[7]C.W. Nan. Magnetoelectric effect in composites of piezoelectric and piezomagnetic phases. *Physical Review B*, 50:6082–6088, 1994.

[8]M. Avellaneda and G. Harsche. Magnetoelectric effect in piezoelectric/magnetostrictive multilayer (2-2) composites. *Journal of Intelligent Material Systems and Structures*, 5:501–513, 1994.

[9]Y. Benveniste. Magnetoelectric effect in fibrous composite with piezoelectric and piezomagnetic phases. *Physical Review B*, 51:16424–16427, 1995.

[10]G. Davì, A. Milazzo, and C. Orlando. Magneto-electro-elastic bimorph analysis by the boundary element method. *Mechanics of Advanced Materials and Structures*, 15:220–227, 2008.

[11]K. Chandrashekhara and A. N. Agarwal. Active vibration control of laminated composite plates using piezoelectric devices: A finite element approach. *Journal of Intelligent Material Systems and Structures*, 4:496–508, 1993.

[12]Q. Luo and L. Tong. High precision shape control of plates using orthotropic piezoelectric actuators. *Finite Elements in Analysis and Design*, 42:1009–1020, 2006.

[13]L.-W. Chen, C.-Y. Lin, and C.-C. Wang. Dynamic stability analysis and control of a composite beam with piezoelectric layers. *Composite Structures*, 56:97–109, 2002.

[14]S. K. Bapanapalli, O. M. Martinez, C. Gogu, B. V. Sankar, R. T. Haftka, and Blosser M. L. Analysis and design of corrugated-core sandwich planels for thermal protection systems of space vehicles. In *Proceedings of 47th AIAA/ASME/ASCE/AHS/ASC Structures, Structural Dynamics, and Materials Conference*, Newport, Rhode Island, May. 1 – 4 2006. AIAA.

[15]N. Okamoto, M. Kusakari, K. Tanaka, H. Inui, M. Yamaguchi, and S. Otani. Temperature dependence of thermal expansion and elastic constants of single crystals of ZrB_2 and the suitability of ZrB_2 as a substrate for GaN film. *Journal of Applied Physics*, 93:88–93, 2003.

[16]N. Noda. Thermal stresses in materials with temperature-dependent properties. *Applied Mechanics Reviews*, 44:383 – 397, 1991.

[17]A. K. Soh and J. X. Liu. On the constitutive equations of magnetoelectroelastic solids. *Journal of Intelligent Material Systems and Structures*, 16:597–602, 2005.

[18]P. C. Y. Lee. A variational principle for the equations of piezoelectromagnetism in elastic dielectric crystals. *Journal of Applied Physics*, 69:4770–4773, 1991.

[19]J. H. He. Variational theory for linear magneto-electro-elasticity. *International Journal of Nonlinear Sciences and Numerical Simulation*, 2:309–316, 2001.

[20]G. Altay and M. C. Dokmeci. Certain hygrothermopiezoelectric multi-field variational principles for smart elastic laminae. *Mechanics of Advanced Materials and structures*, 14:549–562, 2008.

[21]E. Carrera, S. Brischetto, and P. Nali. Variational statements and computational models for multifield problems and multilayered structures. *Mechanics of Advanced Materials and Structures*, 15:182–198, 2008.

[22]A. Jiang and H. Ding. Analytical solutions to magneto-electro-elastic beams. *Structural Engineering and Mechanics*, 18:195–209, 2004.

[23]A. Kumaravel, N. Ganesan, and R. Sethuraman. Steady-state analysis of a three-layered electro-magneto-elastic strip in a thermal environment. *Smart Materials and Structures*, 16:282–295, 2007.

[24]V. L. Berdichevsky. Variational-asymptotic method of constructing a theory of shells. *PMM*, 43:664–687, 1979.

[25]W. Yu, D. H. Hodges, V. Volovoi, and C. E. S. Cesnik. On Timoshenko-like modeling of initially curved and twisted composite beams. *International Journal of Solids and Structures*, 39:5101–5121, 2002.

[26]C. E. S. Cesnik and R. Palacios. Modeling piezocomposite actuators embedded in slender structures. In *Proceedings of the 11th AIAA/ASME/AHS Adaptive Structures Conference*, Norfolk, VA, April 2003. AIAA.

[27]R. Palacios and C. E. S. Cesnik. Cross-sectional analysis of nonhomogeneous anisotropic active slender structures. *AIAA Journal*, 43(12):2624–2638, 2005.

[28]S. Roy, W. Yu, and D. Han. An asymptotically correct classical model for smart beams. *International Journal of Solids and Structures*, 44:8424–8439, 2007.

[29]S. Roy and W. Yu. Dimensional reduction of a piezoelectric composite rod. *European Journal of Mechanics A/Solids*, 28:368–376, 2009.

[30]Q. Wang and W. Yu. A refined model for thermoelastic analysis of initially curved and twisted composite beams. In *Proceedings of 51st AIAA/ASME/ASCE/AHS/ASC Structures, Structural Dynamics, and Materials Conference*, Orlando, FL, Apr. 12 – 15 2010. AIAA.

[31]Q. Wang and W. Yu. Variational asymptotic modeling of multiphysical behavior of smart slender structures. In *Proceedings of 52nd AIAA/ASME/ASCE/AHS/ASC Structures, Structural Dynamics, and Materials Conference*, Denver, CO, April 2010. AIAA.

[32]B. A. Boley and J. H. Weiner. *Theory of Thermal Stresses*. Dover Publications, 1997.